J|A|C|S
ARTICLES

Published on Web 08/06/2008

Morphology Controlled Self-Assembled Nanostructures of Sandwich Mixed (Phthalocyaninato)(Porphyrinato) Europium Triple-Deckers. Effect of Hydrogen Bonding on Tuning the Intermolecular Interaction

Guifen Lu,[†] Yanli Chen,[‡] Yuexing Zhang,[†] Meng Bao,[‡] Yongzhong Bian,[†] Xiyou Li,[†] and Jianzhuang Jiang*,[†]

Department of Chemistry, Shandong University, Jinan 250100, China and Department of Chemistry, University of Jinan, Jinan 250022, China

Received April 22, 2008; E-mail: jzjiang@sdu.edu.cn

Abstract: A series of five novel sandwich-type mixed (phthalocyaninato)(porphyrinato) europium triple-decker complexes with different numbers of hydroxyl groups at the meso-substituted phenyl groups of porphyrin ligand **1**−**5** have been designed, synthesized, and characterized. Their self-assembly properties, in particular the effects of the number and positions of hydroxyl groups on the morphology of self-assembled nanostructures of these triple-decker complexes, have been comparatively and systematically studied. Competition and cooperation between the intermolecular $\pi-\pi$ interaction and hydrogen bonding in the direction perpendicular to the $\pi-\pi$ interaction direction for different compounds were revealed to result in nanostructures with a different morphology from nanoleafs for **1**, nanoribbons for **2**, nanosheets for **3**, and curved nanosheets for **4** and to spherical shapes for **5**. The IR and X-ray diffraction (XRD) results reveal that, in the nanostructures of triple-decker **2** as well as **3**−**5**, a dimeric supramolecular structure was formed through an intermolecular hydrogen bond between two triple-decker molecules, which as the building block self-assembles into the target nanostructures. Electronic absorption spectroscopic results on the self-assembled nanostructures reveal the *H*-aggregate nature in the nanoleafs and nanoribbons formed from triple-deckers **1** and **2** due to the dominant $\pi-\pi$ intermolecular interaction between triple-decker molecules, but the *J*-aggregate nature in the curved nanosheets and spherical shapes of **4** and **5** depending on the dominant hydrogen bonding interaction in cooperation with $\pi-\pi$ interaction among the triple-decker molecules. Electronic absorption and XRD investigation clearly reveal the decrease in the $\pi-\pi$ interaction and increase in the hydrogen bonding interaction among triple-decker molecules in the nanostructures along with the increase of hydroxyl number in the order of **1**−**5**. The present result appears to represent the first effort toward realization of controlling and tuning the morphology of self-assembled nanostructures of sandwich tetrapyrrole rare earth complexes through molecular design and synthesis.

Introduction

Self-assembly of functional organic molecules into well-defined nanostructures due to various noncovalent interactions including $\pi-\pi$ interaction, van der Waals, hydrogen bonding, hydrophilic/hydrophobic, electrostatic, and metal−ligand coordination are important for the development of advanced functional molecular materials as well as nanoscale electronic and optoelectronic devices.[1] On the basis of different noncovalent interactions, a wide variety of nanostructures such as fibers, rods, sheets, cubes, and tubes have been fabricated from various functional molecular materials.[2−5] In particular, nanostructures self-assembled from molecular materials with a conjugated electronic molecular structure have attracted increasing research interests in the field of nanoscience and nanotechnology due to their potential applications in sensors,[6−9] field-effect transistors,[10−12] and photovoltaics.[13−18]

[†] Shandong University.
[‡] University of Jinan.

(1) Elemans, J. A. A. W.; Hameren, R.; van; Nolte, R. J. M.; Rowan, A. E. *Adv. Mater.* **2006**, *18*, 1251–1226.
(2) (a) Hartgerink, J. D.; Beniash, E.; Stupp, S. I. *Science* **2001**, *294*, 1684–1688. (b) Kitamura, T.; Nakaso, S.; Mizoshita, N.; Tochigi, Y.; Shimomura, T.; Moriyama, M.; Ito, K.; Kato, T. *J. Am. Chem. Soc.* **2005**, *127*, 14769–14775.
(3) Schwab, A. D.; Smith, D. E.; Bond-Watts, B.; Johnston, D. E.; Hone, J.; Johnson, A. T.; de Paula, J. C.; Smith, W. F. *Nano Lett.* **2004**, *4*, 1261–1265.
(4) Wang, Z.; Li, Z.; Medforth, C. J.; Shelnutt, J. A. *J. Am. Chem. Soc.* **2007**, *129*, 2440–2441.
(5) (a) Yan, D. Y.; Zhou, Y. F.; Hou, J. *Science* **2004**, *303*, 65–67. (b) Shimizu, T.; Masuda, M.; Minamikawa, H. *Chem. Rev.* **2005**, *105*, 1401–1444. (c) Zhi, L.; Gorelik, T.; Wu, J.; Kolb, U.; Müllen, K. *J. Am. Chem. Soc.* **2005**, *127*, 12792–12793. (d) Hu, J.-S.; Guo, Y.-G.; Liang, H.-P.; Wan, L.-J.; Jiang, L. *J. Am. Chem. Soc.* **2005**, *127*, 17090–17095.
(6) Liu, R.; Holman, M. W.; Zang, L.; Adams, D. M. *J. Phys. Chem. A* **2003**, *107*, 6522–6526.
(7) Holman, M. W.; Liu, R.; Zang, L.; Yan, P.; DiBenedetto, S. A.; Bowers, R. D.; Adams, D. M. *J. Am. Chem. Soc.* **2004**, *126*, 16126–16133.
(8) Sauer, M. *Angew. Chem., Int. Ed.* **2003**, *42*, 1790–1793.
(9) Grimsdale, A. C.; Müllen, K. *Angew. Chem., Int. Ed.* **2005**, *44*, 5592–5629.
(10) Xu, B. Q.; Xiao, X.; Yang, X.; Zang, L.; Tao, N. J. *J. Am. Chem. Soc.* **2005**, *127*, 2386–2387.

 © 2008 American Chemical Society

Investigations have revealed that self-assembly of conjugated molecular systems depends mainly on the intermolecular $\pi-\pi$ interaction in cooperation with other noncovalent interactions, forming nanostructures with different morphologies. As a result, introduction of different functional groups onto the peripheral positions of conjugated molecules has been employed to tune the morphology of self-assembled nanostructures formed via inducing the deformation of a conjugated system from a planar structure and/or introducing additional intermolecular interactions. Yokoyama and co-workers have reported that substituted porphyrin molecules adsorbed on a gold surface form monomers, trimers, tetramers, or extended wirelike structures, each of which corresponds in a predictable fashion to the geometric and chemical nature of the porphyrin substituents that mediate the interactions between individual adsorbed molecules.[19] Zang and co-workers have found that incorporation of dodecyl chains onto the nitrogen atoms of the perylene diimide (PTCDI) ring is beneficial for the formation of nanobelts.[20] In contrast, incorporating two space-demanding nonyldecyl groups onto the same positions of the PTCDI ring interferes with the effective intermolecular $\pi-\pi$ interaction due to the steric hindrance, leading to the formation of nanospheres via a self-assembly process. Comparative studies on the self-assembly behavior between dodecyloxy-substituted PTCDI and dodecylthio-substituted PTCDI revealed that incorporation of thiododecyl chain(s) onto the bay positions of the perylene ring of PTCDI induces the deformation of the conjugated PTCDI ring from the planar system and therefore interferes with the effective $\pi-\pi$ interaction between PTCDI molecules, preventing the self-assembly from growing along one dimension and resulting in the formation of spherical nanoparticles on the basis of the self-assembly process of di(thiododecyl)-substituted PTCDI.[21]

As the typical representatives of functional molecular materials with large conjugated electronic molecular structure, porphyrins and phthalocyanines have been extensively studied over the past century due to their wide range of biological relevance and industrial applications.[22] In recent years, the self-assembly behavior and nanostructures of these tetrapyrrole compounds have also started to attract extensive research interests because of their potential applications in diverse fields. For example, hollow capsules with potential application as drug delivery agents were produced using a phase transfer method depending on the strong $\pi-\pi$ interaction between porphyrin molecules.[23] Nanotubes with photocatalytic activity were synthesized by electrostatic force between two oppositely charged porphyrins.[24] Investigation over the organogel formation properties of a series of porphyrins with amide groups as peripheral hydrogen bonding sites indicates that the aggregation mode of porphyrin stacks can be tuned by the hydrogen bonding interaction.[25] Cooperation between the $\pi-\pi$ interaction and hydrogen bondings among the molecules of phthalocyanine copper complexes decorated with optically active diol units induces the formation of fibrous assemblies.[26] Phthalocyanines appended with substituted crown-ether moieties have been readily self-assembled into long fibers.[27] However, it must be pointed out that self-assembly of functional molecules into a prerequisite nanostructure with desirable dimension and morphology *via* controlling and optimizing the intermolecular interaction still remains a great challenge for chemists and material scientists.

Associated with their potential applications in materials science and molecular electronics, sandwich phthalocyaninato and/or porphyrinato rare earth complexes have attracted great attention.[28] The presence of two or three tetrapyrrole rings in one molecule with a sandwich molecular structure of these compounds provides much more possibilities to tune the intermolecular interactions due to the versatile possible substitution positions in different tetrapyrrole rings. It is therefore worth investigating the self-assembling properties of sandwich tetrapyrrole rare earth complexes in terms of both potential applications and theoretical importance. However, very little has been done in this direction. Very lately, using a template method, a sandwich (phthalocyaninato)(porphyrinato) europium double-decker compound has been fabricated into nanotubes by this group.[29] This, to the best of our knowledge, represents the sole example of nanostructures fabricated from sandwich tetrapyrrole rare earth complexes. In the present paper, we describe the design, synthesis, characterization, and self-assembly properties of a series of novel sandwich-type mixed (phthalocyaninato)(porphyrinato) europium triple-decker complexes, namely $Eu_2(Pc)_2(TBPP)$ (Pc = dianion of phthalocyanine, TBPP = dianion of 5,10,15,20-tetra(4-*tert*-butylphenyl)porphyrin] (**1**), $Eu_2(Pc)_2$[T(OH)PP] [T(OH)PP = dianion of 5-(4-hydroxyphenyl)-10,15,20-tris(4-*tert*-butylphenyl)porphyrin] (**2**), $Eu_2(Pc)_2$[*trans*-$T(OH)_2PP$] [*trans*-$T(OH)_2PP$ = dianion of 5,15-di(4-hydroxyphenyl)-10,20-di(4-*tert*-butylphenyl)porphyrin] (**3**), $Eu_2(Pc)_2$[*cis*-$T(OH)_2PP$] [*cis*-$T(OH)_2PP$ = dianion of 5,10-di(4-hydroxyphenyl)-15,20-di(4-*tert*-butylphenyl)porphyrin] (**4**), and

(11) Li, X.; Xu, B. Q.; Xiao, X.; Yang, X.; Zang, L.; Tao, N. J. *Faraday Discuss.* **2006**, *131*, 111–120.
(12) (a) Chen, Y.; Su, W.; Bai, M.; Jiang, J.; Li, X.; Liu, Y.; Wang, L.; Wang, S. *J. Am. Chem. Soc.* **2005**, *127*, 15700–15701. (b) Li, R.; Ma, P.; Dong, S.; Zhang, X.; Chen, Y.; Li, X.; Jiang, J. *Inorg. Chem.* **2007**, *46*, 11397–11404.
(13) Schmidt-Mende, L.; Fechtenkötter, A.; Müllen, K.; Moons, E.; Friend, R. H.; MacKenzie, J. D. *Science* **2001**, *293*, 1119–1122.
(14) Gregg, B. A. *J. Phys. Chem. B* **2003**, *107*, 4688–4698.
(15) Gregg, B. A. *J. Phys. Chem.* **1996**, *100*, 852–859.
(16) Tamizhmani, G.; Dodelet, J. P.; Côté, R.; Gravel, D. *Chem. Mater.* **1991**, *3*, 1046–1053.
(17) Li, Y.; Xiao, S.; Li, H.; Li, Y.; Liu, H.; Lu, F.; Zhuang, J.; Zhu, D. *J. Phys. Chem. B* **2004**, *108*, 6256–6260.
(18) Peeters, E.; Van Hal, P. A.; Meskers, S. C. J.; Janssen, R. A. J.; Meijer, E. W. *Chem.—Eur. J.* **2002**, *8*, 4470–4474.
(19) Yokoyama, T.; Yokoyama, S.; Kamikado, T.; Yoshishige Okuno, Y.; Mashiko, T. *Nature* **2001**, *413*, 619–621.
(20) Balakrishnan, K.; Datar, A.; Naddo, T.; Huang, J.; Oitker, R.; Yen, M.; Zhao, J.; Zang, L. *J. Am. Chem. Soc.* **2006**, *128*, 7390–7398.
(21) Su, W.; Zhang, Y.; Zhao, C.; Li, X.; Jiang, J. *ChemPhysChem* **2007**, *8*, 1857–1862.
(22) (a) Hamza, I. *ACS Chem. Biol.* **2006**, *1*, 627–629. (b) Lo, P.-C.; Chan, C. M. H.; Liu, J.-Y.; Fong, W.-P.; Ng, D. K. P. *J. Med. Chem.* **2007**, *50*, 2100–2107. (c) Vanyúr, R.; Héberger, K.; Jakus, J. *J. Chem. Inf. Comput. Sci.* **2003**, *43*, 1829–1836.
(23) Li, Y.; Li, X.; Li, Y.; Liu, H.; Wang, S.; Gan, H.; Li, J.; Wang, N.; He, X.; Zhu, D. *Angew. Chem., Int. Ed.* **2006**, *45*, 3639–3643.
(24) Wang, Z.; Medforth, C. J.; Shelnutt, J. A. *J. Am. Chem. Soc.* **2004**, *126*, 15954–15955.
(25) Shirakawa, M.; Kawano, S.-i.; Fujita, N.; Sada, K.; Shinkai, S. *J. Org. Chem.* **2003**, *68*, 5037–5044.
(26) Kimura, M.; Muto, T.; Takimoto, H.; Wada, K.; Ohta, K.; Hanabusa, K.; Shirai, H.; Kobayash, N. *Langmuir* **2000**, *16*, 2078–2082.
(27) Engelkamp, H.; Middelbeek, S.; Nolte, R. J. M. *Science* **1999**, *284*, 785–788.
(28) (a) For example, see: Jiang, J.; Ng, D. K. P. *Acc. Chem. Res*., invited and submitted. (b) Jiang, J.; Bao, M.; Rintoul, L.; Arnold, D. P. *Coord. Chem. Rev.* **2006**, *250*, 424–448. (c) Jiang, J.; Kasuga, K.; Arnold, D. P. In *Supramolecular Photosensitive and Electroactive Materials*; Nalwa, H. S., Ed.; Academic Press: New York, 2001; Chapter *2*, pp 113−210. (d) Ng, D. K. P.; Jiang, J. *Chem. Soc. Rev.* **1997**, *26*, 433–442. (e) Yoshimoto, S.; Sawaguchi, T.; Su, W.; Jiang, J.; Kobayashi, N. *Angew. Chem., Int. Ed.* **2007**, *46*, 1071–1074. (f) Ye, T.; Takami, T.; Wang, R.; Jiang, J.; Weiss, P. S. *J. Am. Chem. Soc.* **2006**, *128*, 10984–10985.
(29) Li, Q.; Li, Y.; Liu, H.; Chen, Y.; Wang, X.; Zhang, Y.; Li, X.; Jiang, J. *J. Phys. Chem. C* **2007**, *111*, 7298–7301.

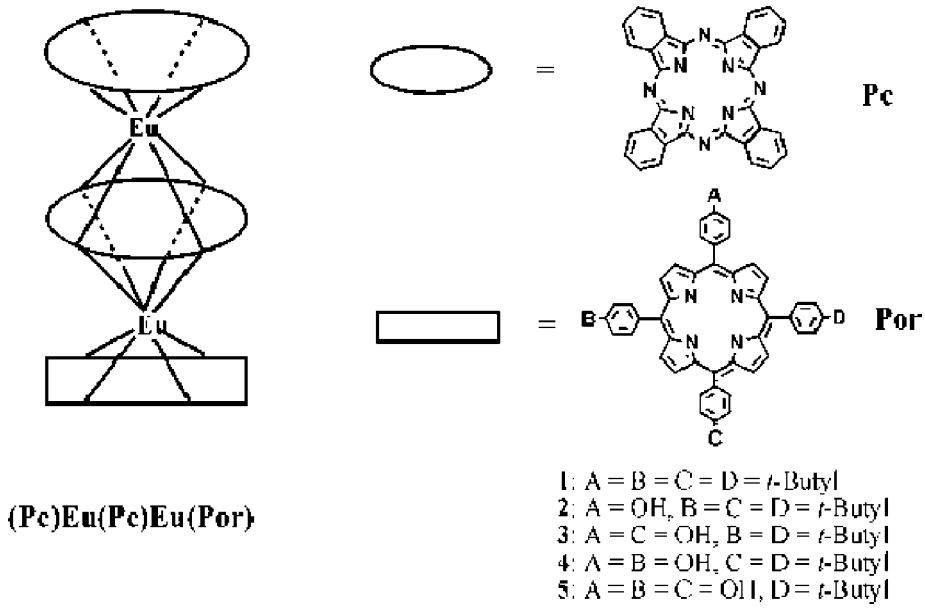

Figure 1. Schematic molecular structures of the mixed (phthalocyaninato)(porphyrinato) europium triple-decker complexes **1**−**5**.

Table 1. Analytical and Mass Spectroscopic Data for the Triple-Decker Complexes **1**−**5**[a]

compound	yield (%)	M^+ (m/z)[a,b]	analysis (%)[a] C	H	N
$Eu_2(Pc)_2$(TBPP) (**1**)	42	2166.6 (2166.1)	67.13 (67.18)	4.42 (4.19)	12.40 (12.59)[c]
$Eu_2(Pc)_2$[T(OH)PP] (**2**)	40	2127.7 (2126.0)	64.18 (64.72)	4.14 (3.81)	12.11 (12.48)[c]
$Eu_2(Pc)_2$[trans-T$(OH)_2$PP] (**3**)	38	2085.1 (2085.9)	64.96 (64.56)	3.77 (3.56)	13.05 (12.90)[c]
$Eu_2(Pc)_2$[cis-T$(OH)_2$PP] (**4**)	26	2086.0 (2085.9)	64.39 (63.72)	3.94 (3.52)	12.20 (12.70)[c]
$Eu_2(Pc)_2$[T$(OH)_3$PP] (**5**)	25	2045.9 (2045.8)	63.69 (63.52)	3.59 (3.25)	12.86 (13.14)[c]

[a] Calculated values given in parentheses. [b] By MALDI-TOF mass spectrometry. The value corresponds to the most abundant isotopic peak of the molecular ion (M^+). [c] For **1**·$^1/_2CHCl_3$ **2**·$CHCl_3$, **3**·$^3/_4CHCl_3$, **4**·$CHCl_3$, and **5**·$^3/_4CHCl_3$.

$Eu_2(Pc)_2$[T$(OH)_3$PP] [T$(OH)_3$PP = dianion of 5,10,15-tris(4-hydroxyphenyl)-20-(4-*tert*-butylphenyl)porphyrin] (**5**), Figure 1. Introduction of different numbers of hydroxyl groups onto the meso-substituted phenyl groups of porphyrin ligand in the triple-decker molecule leads to the formation of nanostructures with different morphologies, clearly revealing the effect of hydrogen bonding interaction in tuning the intermolecular interaction between triple-decker molecules in the self-assembly process. This not only represents the first effort toward understanding the relationship between the molecular structure and corresponding nanostructures of sandwich tetrapyrrole rare earth compounds but also provides information on preparing self-assembled nanostructures with a controlled molecular packing conformation and morphology through molecular design and synthesis.

Results and Discussion

Molecular Design, Synthesis, and Characterization. Composed of two or three tetrapyrrole ligands connected by one or two rare earth metal ion(s), phthlaocyaninato and/or porphyrinato rare earth complexes with a special sandwich molecular structure are typically large conjugated molecular electronic structures. As expected, the dominant intermolecular interaction among sandwich tetrapyrrole rare earth molecules is $\pi-\pi$ interaction. Tuning the intermolecular interaction of sandwich tetrapyrrole rare earth molecules can therefore be reached by introducing an additional molecular interaction through introducing functional groups onto the peripheral positions of phthalocyanine and/or porphyrin rings. On the basis of consideration of the directional-specific character of hydrogen bonding, different numbers of hydroxyl groups have been incorporated onto the meso-substituted phenyl groups at the porphyrin ligand of the sandwich mixed (phthalocyaninato)(porphyrinato) europium molecule as hydrogen bonding sites, Figure 1.

There are several possible synthetic pathways to preparing mixed (phthalocyaninato)(porphyrinato) rare earth(III) triple-decker complexes.[30] The most commonly used method is the so-called one-pot reaction with H_2Por, M$(Pc)_2$, and Eu$(acac)_3$·$n H_2O$ as starting materials.[30c] In the present study, the target triple-decker complexes **1**-**5** were obtained with good yields from the reaction between corresponding metal free porphyrin H_2TBPP/H_2T$(OH)_n$PP (n = 1, 2, 3) and Eu$(Pc)_2$ in the presence of Eu$(acac)_3$·$n H_2O$ in refluxing TCB. However, it is worth noting that effort using H_2T$(OH)_4$PP failed to give $Eu_2(Pc)_2$[T$(OH)_4$PP] probably due to the very limited solubility of H_2T$(OH)_4$PP in TCB. Satisfactory elemental analysis results were obtained for all the newly prepared mixed ring triple-decker complexes after repeated column chromatographic purification and recrystallization, Table 1. The MALDI-TOF mass spectra of **1**−**5** showed an intense cluster corresponding to the molecular

(30) (a) Kirin, I. S.; Moskalev, P. N.; Makashev, Y. A.; Russ, J. *Inorg. Chem.* **1965**, *10*, 1065–1066. (b) Buchler, J. W.; Ng, D. K. P. In *The Porphyrin Handbook*; Kadish, K. M., Smith, K. M., Guilard, R., Eds.; Academic Press: San Diego, 2000; Vol. 3, pp 245−294. (c) Sun, X.; Cui, X.; Arnold, D. P.; Choi, M. T. M.; Ng, D. K. P.; Jiang, J. *Eur. J. Inorg. Chem.* **2003**, *8*, 1555–1561. (d) Sun, X.; Li, R.; Wang, D.; Dou, J.; Zhu, P.; Lu, F.; Ma, C.; Choi, Ch-F.; Cheng, D. Y. Y.; Ng, D.K. P.; Kobayashi, N.; Jiang, J. *Eur. J. Inorg. Chem.* **2004**, *19*, 3806–3813.

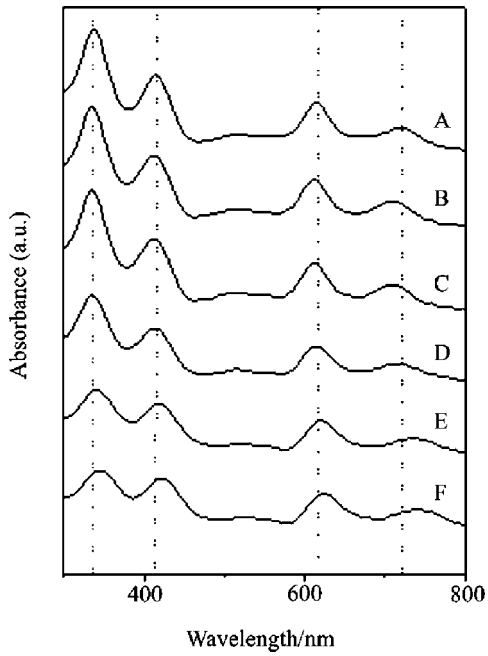

Figure 2. Electronic absorption spectra of $Eu_2(Pc)_2$(TBPP) (**1**) in $CHCl_3$ (5×10^{-6} mol L^{-1}) (A) and **1**−**5** in *n*-hexane (5×10^{-6} mol L^{-1}) (B−F).

ion (M^+), and the data are also given in Table 1. These new sandwich triple-decker compounds were also characterized with a range of spectroscopic methods. Table S1 (Supporting Information) collects the ^{1}H NMR spectroscopic data of the triple-deckers **1**−**5** in $CDCl_3$. The spectral assignments could easily be reached on the basis of the integration and multiplicity of the signals and with reference to the results on $Eu_2(Pc)_2$-(TBPP) (**1**) and $Eu_2(Pc)_2$(TClPP).[30d]

Electronic Absorption Spectra in Solutions. The electronic absorption spectra of the mixed ring triple-decker complexes **1**−**5** in $CHCl_3$ are recorded, and the data are compiled in Tables S2 (Supporting Information). As revealed, all five of these triple-decker complexes $Eu_2(Pc)_2$(TBPP) (**1**) and $Eu_2(Pc)_2$[T(OH)$_n$PP] (n = 1, 2, 3) (**2**−**5**), regardless of the number of hydroxyl groups at the meso-substituted phenyl groups of porphyrin ring, dissolved in $CHCl_3$ show just the same feature in their electronic absorption spectra, revealing the nonaggregated molecular spectroscopic nature of all of these five compounds in $CHCl_3$. Figure 2A displays the electronic absorption spectrum of $Eu_2(Pc)_2$(TBPP) (**1**) as the typical representative of the series of mixed-ring triple-decker complexes in $CHCl_3$. In line with that of analogous $M_2(Pc)_2$(TClPP) (M = Nd, Gd, Dy),[30d] the absorptions at ∼335 and 415 nm can be attributed to the phthalocyanine and porphyrin Soret bands, respectively, while the strong absorptions at 615 and 720 nm can be attributed to their Q bands.

The electronic absorption spectra of the series of five triple-decker complexes in *n*-hexane (5×10^{-6} mol L^{-1}) are also recorded and given in Figure 2, which are significantly different from the spectrum of $Eu_2(Pc)_2$(TBPP) (**1**) dissolved in $CHCl_3$. Nevertheless, significant differences also exist in the electronic absorption spectrum among the five compounds in *n*-hexane, indicating different aggregation states formed from different triple-deckers. As shown in Figure 2, the phthalocyanine and porphyrin Soret bands at 335 and 415 nm in $CHCl_3$ for both $Eu_2(Pc)_2$(TBPP) (**1**) and $Eu_2(Pc)_2$[T(OH)PP] (**2**) without and with only one hydroxyl group at the meso-substituted phenyl groups of porphyrin ring take a blue shift to 333 and 410 nm, respectively, when dispersed in *n*-hexane, and the Q absorptions at 615 and 720 nm in chloroform blue-shifted to 610 and 710 nm in *n*-hexane. When two hydroxyl groups are introduced onto the two opposite meso-substituted phenyl groups of the porphyrin ring of the triple-decker molecules, aggregation of triple-decker molecules of $Eu_2(Pc)_2$[trans-T(OH)$_2$PP] (**3**) in *n*-hexane leads to a blue shift in one Q absorption band from 720 nm in chloroform to 715 nm in *n*-hexane with all the other absorption bands remaining unshifted, Figure 2. However, introduction of two hydroxyl groups onto the two neighboring meso-substituted phenyl groups of the porphyrin ligand in the triple-decker molecule induces a red-shift in all the Soret and Q absorptions for $Eu_2(Pc)_2$[cis-T(OH)$_2$PP] (**4**), from 335, 415, 615, and 720 nm in $CHCl_3$ to 340, 418, 620, and 735 nm in *n*-hexane, Figure 2, indicating the effect of the positions of the hydroxyl groups, actually the hydrogen-bonding motif, on the molecular packing conformation in aggregates due to the directional-specific character of hydrogen bonding. Along with introducing three hydroxyl groups onto the three meso-attached phenyl groups in the porphyrin ligand of $Eu_2(Pc)_2$[T(OH)$_3$PP] (**5**), aggregation of triple-decker molecules of this compound in *n*-hexane leads to an even further red shift for all the Soret and Q absorption bands to 343, 420, 625, and 740 nm, Figure 2. On the basis of Kasha's exciton theory,[31] blue shifts in the main absorption bands of triple-deckers **1** and **2** upon aggregation are typically a sign of the effective $\pi-\pi$ interaction between triple-decker molecules, indicating the formation of an *H* aggregate from these two compounds in *n*-hexane. In contrast, the red-shifted absorption bands in the electronic absorption spectra of triple-deckers **4** and **5** upon aggregation in *n*-hexane imply the triple-decker molecules of these complexes are enforced to adopt the *J* aggregation mode. These results indicate the dominant role of $\pi-\pi$ interaction between the molecules of triple-decker complexes **1** and **2** but of hydrogen bonding for **4** and **5**. As for triple-decker **3**, the electronic absorption spectroscopic result appears to give no hint about the dominant intermolecular interaction in the aggregates formed in *n*-hexane. In addition, with the aggregate of $Eu_2(Pc)_2$(TBPP) (**1**) in *n*-hexane as reference, comparison among the electronic spectra of **1**−**5** in *n*-hexane indicates that, along with the increase of hydroxyl number in the meso-substituted phenyl groups of porphyrin ligand, both the phthalocyanine and porphyrin Soret and Q bands continuously shift to the lower energy side in the same order, revealing the effect of the hydrogen-bonding interaction among hydroxyl groups on tuning the intermolecular interaction of triple-decker molecules and in turn the aggregation mode. Furthermore, comparison in the aggregate electronic absorption spectra between **3** and **4**, with two hydroxyl groups at two opposite and neighboring meso-substituted phenyl groups of porphyrin ring, respectively, reveals the effect of hydroxyl positions on tuning the intermolecular interaction and in turn the molecular packing mode in the aggregate due to the directional-specific character of hydrogen bonding.

IR Spectral Spectra. The IR spectra of the self-assembled nanostructures of **1**−**5** obtained are shown in Figure S1 (Supporting Information). In the IR spectra of triple-deckers **2**−**5**, two relatively broad bands appearing in the range 3391−3471 cm^{-1}, which are absent from that for **1**, are assigned

(31) Kasha, M.; Rawls, H. R.; EI-Bayoumi, M. A. *Pure Appl. Chem.* **1965**, *11*, 371–392.

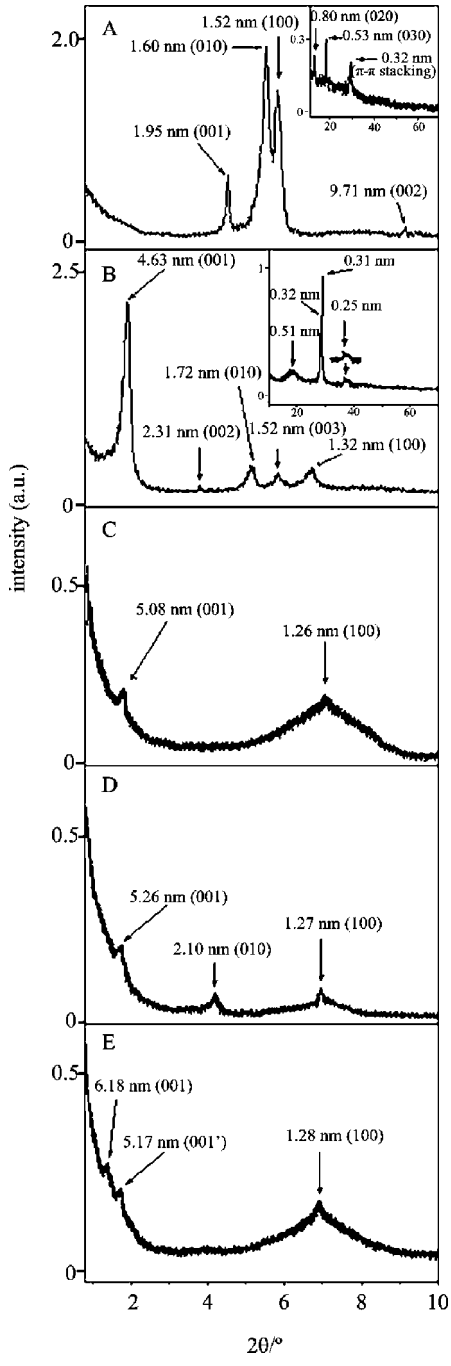

Figure 3. XRD profiles of the aggregates of compounds **1**−**5** (A−E).

to the hydrogen bonding stretching vibration.[26,32] This is in line with the X-ray diffraction (XRD) result as detailed below, indicating the significant effect of the hydrogen-bonding interaction on the formation of molecular aggregates of **2**−**5**.

X-ray Diffraction Patterns. The nanostructures of the series of triple-decker complexes were fabricated by injecting a small volume of solution of **1**−**5** in chloroform solution (1 mM) into a large volume of *n*-hexane. The internal structure of self-assembled nanostructures of these complexes was investigated by XRD analysis, Figure 3. As shown in Figure 3A, in the low angle range, the XRD diagram of the nanoleafs formed from compound **1** shows a strong refraction peak at $2\theta = 4.53°$ (corresponding to1.95 nm) along with one weaker second-order refraction at 0.97 nm, which are ascribed to the refractions from the (001) and (002) planes. In addition, the XRD pattern also displays two more well-defined peaks at 1.60 and 1.52 nm, respectively, originating from the (010) and (100) planes.[33] The (010) plane gives its higher order refractions at 0.80 (020) and 0.53 (030) nm, respectively, in the wide angle range of the XRD pattern. These diffraction results could be assigned to the refractions from a rectangular lattice with cell parameters $a =$ 1.95 nm, $b = 1.60$ nm, $c = 1.52$ nm, Figure S2 (Supporting Information). As can be seen from Figure S2A (Supporting Information), the dimensional size for a triple-decker molecule of $Eu_2(Pc)_2$(TBPP) (**1**) is 1.52 nm (width) × 0.90 nm (height) using PCMODEL for windows Version 6.0, Serena Software. According to the XRD result and the simulated triple-decker molecular structure, the unit cell consisting of two triple-decker molecules is given for compound **1**, Figure S2B (Supporting Information). It is worth noting that, in the wide angle region, the nanoleaf XRD pattern of this compound presents additional refraction at 0.32 nm, which is attributed to the stacking distance between tetrapyrrole cores of neighboring triple-decker molecules along the direction perpendicular to the tetarpyrrole rings.[26,32−35]

As shown in Figure 3B, in the low angle range, the XRD diagram of the nanoribbons formed from compound **2** shows a comparatively strong and sharp refraction peak at 4.63 nm along with two weaker but still narrow refractions at 2.31 and 1.52 nm, respectively, which are ascribed to the refractions from the (001), (002), and (003) planes. In addition, the XRD pattern also displays two more well-defined peaks at 1.72 and 1.32 nm, respectively, originating from the (010) and (100) planes.[33] These diffraction results could be assigned to the refractions from a rectangular lattice with cell parameters $a = 4.63$ nm, b $= 1.32$ nm, $c = 1.72$ nm, Figure 4. It is worth noting that, in the wide angle region, the XRD pattern presents two sharp refractions at 0.31 and 0.32 nm, respectively, and two relatively wide refractions at 0.51 and 0.25 nm. As indicated by the IR spectroscopic result of the self-assembled nanoribbons obtained from triple-decker **2**, Figure S1 (Supporting Information), two relatively broad bands appearing at 3391 and 3471 cm^{-1} due to the hydrogen bonding stretching vibration indicate the formation of a dimeric supramolecular structure through the formation of an intermolecular hydrogen bond between the hydroxyl groups of triple-decker molecules of $Eu_2(Pc)_2$-[T(OH)PP] (**2**). In other words, during the molecular self-assembly process of this compound, a dimeric supramolecular structure was formed first through an intermolecular hydrogen bond between two triple-decker molecules, which then as the building block further self-assembles into the target nanoribbons (as detailed below) depending mainly on the $\pi-\pi$ interaction between tetrapyrrole rings of triple-decker molecules. This seems also true for triple-deckers **3**−**5**. As can be seen from Figure 4A and 4B, the dimensional size for a dimeric supramolecular structure formed from two triple-decker molecules of $Eu_2(Pc)_2$[T(OH)PP] (**2**) due to the formation of an intermolecular hydrogen bond through hydroxyl groups obtained from the

(32) Kimura, M.; Kuroda, T.; Ohta, K.; Hanabusa, K.; Shirai, H.; Kobayashi, N. *Langmuir* **2003**, *19*, 4825–4830.
(33) Minch, B. A.; Xia, W.; Donley, C. L.; Hernandez, R. M.; Carter, C.; Carducci, M. D.; Dawson, A.; O'Brien, D. F.; Armstrong, N. R. *Chem. Mater.* **2005**, *17*, 1618–1627.
(34) Belarbi, Z.; Sirlin, C.; Simon, J.; Andre, J. J. *J. Phys. Chem.* **1989**, *93*, 8105–8110.
(35) Kimura, M.; Wada, K.; Ohta, K.; Hanabusa, K.; Shirai, H.; Kobayashi, N. *J. Am. Chem. Soc.* **2001**, *123*, 2438–2439.

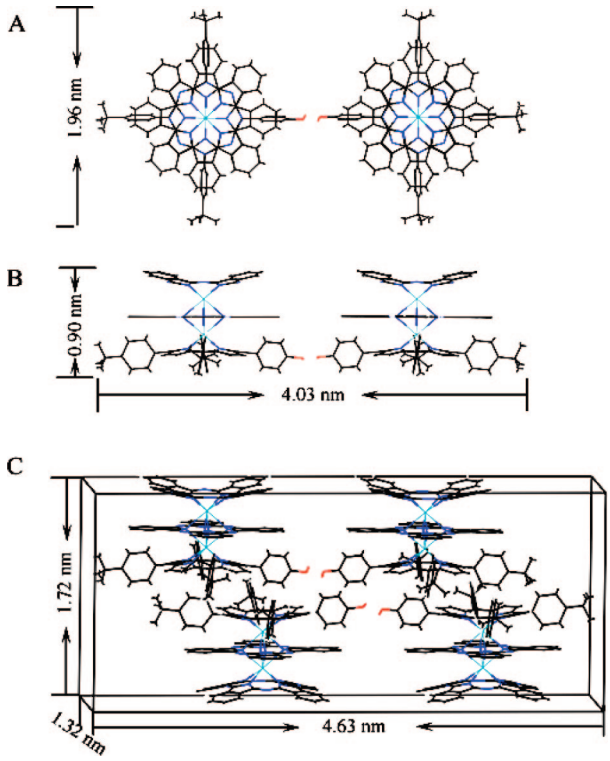

Figure 4. Schematic representation of the unit cell in the aggregate of $Eu_2(Pc)_2[T(OH)PP]$ (**2**). The blue line indicates the coordination bonds between the central metal ion and the sandwich tetrapyrrole ligands. The cyan stands for the metal ion while the red part is the hydroxyl groups.

energy minimized molecular structure is 4.03 nm (length) × 1.96 nm (width) × 0.90 nm (height) using PCMODEL for windows Version 6.0, Serena Software. In a unit cell consisting of two dimeric supramolecular structure building blocks with cell parameters $a = 4.63$ nm, $b = 1.32$ nm, $c = 1.72$ nm, the two sharp diffraction peaks at 0.31 and 0.32 nm for the nanoribbons of **2** correspond to the stacking distance between phthalocyanine−phthalocyanine and porphyrin−porphyrin cores, respectively, of different triple-decker molecules along the direction perpendicular to the phthalocyanine and porphyrin rings, while the relatively wide refractions at 0.51 and 0.25 nm correspond to the distance between the two neighboring supramolecular dimer building blocks[32,34] and the distance between hydrogen bonding hydroxyl oxygens in the dimer.[26] It is worth noting that Kimura and co-workers have reported that the distance between hydrogen bonding hydroxyl oxygens in the self-assembled nanostructure of phthalocyanine compound was 0.26 nm.[26] As shown in Figure 4C, such a unit cell consisting of two dimeric supramolecular structures of **2** is in good accordance with that derived from the XRD experimental result in terms of all corresponding lattice parameters.

The XRD patterns of self-assembled nanostructures of **3**, **4**, and **5** show a weak peak at 5.08, 5.26, and 6.18 nm, respectively, Figure 3C−E. This corresponds with the (001) refraction of nanoribbons of compound **2** appearing at 4.63 nm. The increase of this lattice constant in the order of **2**, **3**, **4**, and **5** indicates the increasing effect of the hydrogen bonding interaction on the formation of the aggregate of these triple-decker complexes in the same order, suggesting the change in the dominant intermolecular interaction from a $\pi-\pi$ interaction to hydrogen bondings in the direction perpendicular to the $\pi-\pi$ interaction direction in the same order. Another common weak and broad refraction observed in the XRD patterns of the self-assembled nanostructures of **3**, **4**, and **5** appears at 1.26, 1.27, and 1.28 nm, respectively, which is in line with the (100) refraction at 1.32 nm for the nanoribbons of **2**. This value is actually corresponding with the diagonal dimension of the core of the rigid phthalocyanine ring, 1.32 nm.[36] However, for compound **3** with two hydroxyl groups attached at the opposite meso-substituted phenyl groups of porphyrin ligand, the (010) refraction observed at 1.72 nm for the nanostructures of **2** was absent, suggesting the lack of long-range periodicity along this direction in the self-assembled nanostructures of this triple-decker complex, indicating the lack of effective intermolecular $\pi-\pi$ interaction among triple-decker molecules. As a consequence, growth in this direction during the self-assembly process is limited or prohibited. This is also true for compound **5**. As for triple-decker **4** with two neighboring hydroxyl groups at the meso-substituted phenyl groups of porphyrin ligand, the lattice parameter along the [010] direction is 2.10 nm. Obviously, in the self-assembled nanostructures with long-range periodicity along the [010] direction as revealed for triple-deckers **1**, **2**, and **4**, the lattice parameter in this direction increases from 1.60 nm for **1**, to 1.72 nm for **2**, and to 2.10 nm for **4**, suggesting that the intermolecular $\pi-\pi$ interaction between triple-decker molecules gradually decreases in the same order. This is in line with the conclusion resulting from the electronic absorption spectroscopic properties as detailed above. As a total result, during the self-assembly process, two triple-decker molecules for **2**−**5** with hydroxyl groups at the meso-substituted phenyl groups of the porphyrin ligand first form a dimeric supramolecular structure through intermolecular hydrogen bonding, which then as the building block further self-assembles into the target nanostructures depending on cooperation between the $\pi-\pi$ interaction among tetrapyrrole rings of triple-decker molecules and the hydrogen bonding interaction in the direction perpendicular to the $\pi-\pi$ interaction direction.

It is worth mentioning that, for the nanospherical shapes of triple-decker **5**, in addition to the major (001) diffraction peak at 6.18 nm, another refraction peak (001′) at 5.17 nm was also observed in the same region, indicating the formation of an oblique (distorted rectangular) phase in addition to the normal one.[37]

Morphology of the Aggregates. The morphology of the aggregates formed was examined by scanning electron microscopy (SEM). Samples were prepared by casting a drop of sample solution onto a carbon-coated grid. The SEM images of aggregates of **1**−**5** were shown in Figures 5 and 6, respectively. As shown in Figure 5A, depending mainly on the intermolecular $\pi-\pi$ interaction in cooperation with the van der Waals interaction, triple-decker molecules of compound **1** self-assemble into nanostructures with a leaf morphology several micrometer long and 500 nm wide. As displayed in Figures 5B and 6, triple-decker molecules of compound **2** self-assemble into nanostructures with a ribbonlike morphology, with long, flexible, and rather thin fibrils (around 30 nm thick) forming the one-dimensional (1D) ribbonlike bundles. The hydroxyl group attached at the porphyrin ring of compound **2** connects two triple-decker molecules to form a supramolecular dimeric building block through intermolecular hydrogen bonding, which is expected to strengthen the $\pi-\pi$ interaction between the

(36) Kobayashi, T; Isoda, S. *J. Mater. Chem.* **1993**, *3*, 1–14.
(37) (a) Petritsch, K.; Friend, R. H.; Lux, A.; Rozenberg, G. G.; Moratti, S. C.; Holmes, A. B. *Synth. Met.* **1999**, *102*, 1776–1777. (b) *Handbook of Liquid Crystals*; Demus, D., Goodby, J., Gray, G. W., Spiess, H.-W., Eds.; Wiley-VCH: New York, 1998; Vol. 1: Fundamentals.

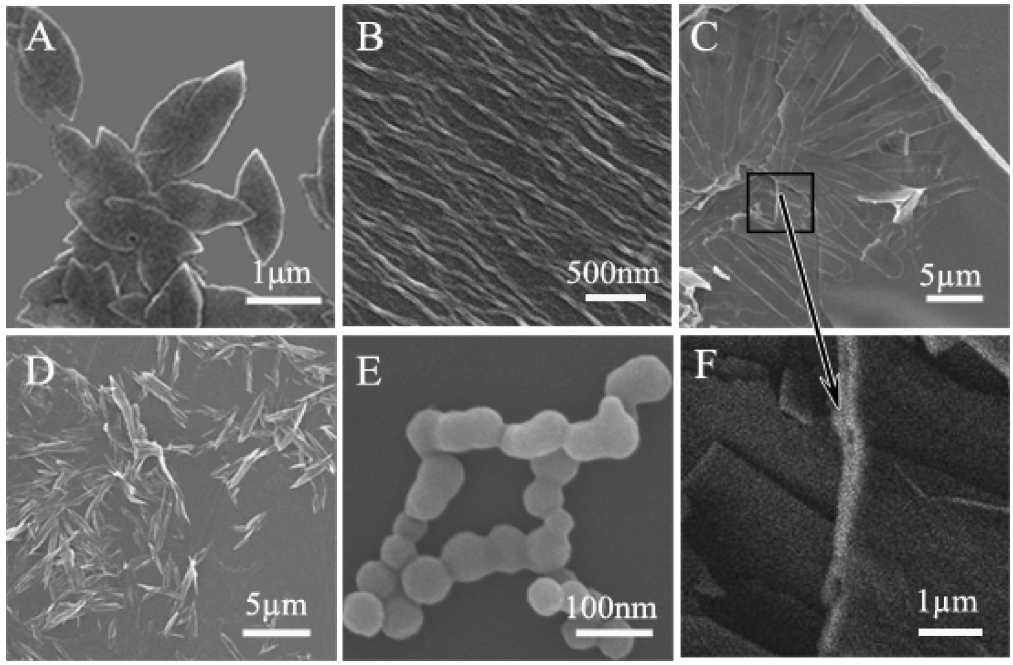

Figure 5. SEM images of nanostructures of compounds **1**−**5** (A−E) and a zoom-in image of the rectangle part in C (F).

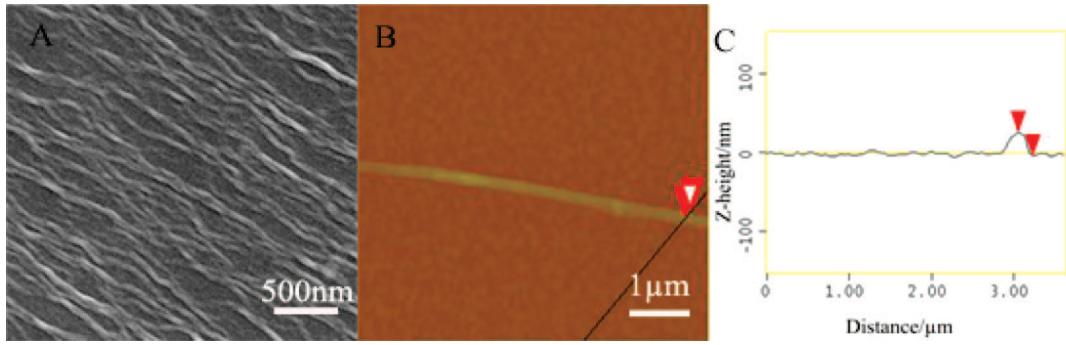

Figure 6. (A) SEM image of nanoribbons (gold-stained) cast on carbon film. (B) High-magnification of AFM image over a single nanoribbon. (C) Z-height line scan profile over a single nanoribbon; tapping mode.

dimeric building block relative to the monomeric species because of the synergetic effect of the two large aromatic molecules.[38] The reinforced $\pi-\pi$ interaction drove the dimeric building block to grow in one direction, leading to the formation of ribbonlike aggregates. The one-dimensional nanoribbons formed from compound **2** display uniform size and orientation, which implies greater intermolecular order. This is favorable for the device applications in photovoltaics and field effect transistors.[39] Along with increasing another hydroxyl group at the opposite meso-substituted phenyl group of porphyrin ring, self-assembly of the triple-decker molecules of **3** results in nanostructures with a two-dimensional sheetlike morphology with a ca. 1 μm width and 10 μm length, Figure 5C. A zoom-in image of the nanosheet (Figure 5F) shows evidence for layered growth. Several thin nanosheets are combined together, forming an extended sheet with a micrometer size. This morphology can be attributed to the introduction of an additional hydroxyl group at the opposite position, which provides another growing direction for the aggregates along the direction of unlimited intermolecular hydrogen bonding besides the $\pi-\pi$ interaction direction. The further increase in the number of the hydroxyl groups at the neighboring meso-substituted phenyl group of the porphyrin ring in the triple-decker molecules induces the formation of self-assembled nanostructures with a curved sheetlike morphology with a ca. 500 nm width and 7 μm length for **4**, Figure 5D. Unlike the situation of triple-decker **3**, the curved nanosheets of **4** exist as independent structures without combining together. It is noteworthy again that XRD results clearly reveal the lack of long-range periodicity along the [010] direction for the nanosheets formed from triple-decker compound **3** but the presence of, despite weakened, long-range periodicity in the same direction for the nanostructures of complex **4**. More interestingly, further increase in the number of hydroxyl groups at the meso-substituted phenyl groups of porphyrin ring in triple-decker compound **5** leads to further change in the morphology of self-assembled nanoscale aggregates. As shown in Figure 5E, the molecular assembly of compound **5** is an approximately spherical shape with an average diameter of ~50 nm. These results reveal that the hydrogen bonding interaction in addition to the $\pi-\pi$ stacking between neighboring molecules plays an important role in controlling and tuning the morphology of aggregates (nanostructures) of these triple-decker compounds in the self-assembly process via

(38) Hoeben, F. J. M.; Jonkheijm, P.; Meijer, E. W.; Schenning, A. P. H. J. *Chem. Rev.* **2005**, *105*, 1491–1546.
(39) Babel, A.; Jenekhe, S. A. *J. Am. Chem. Soc.* **2005**, *125*, 13656–13657.

tuning the intermolecular interaction. The increasing hydrogen bonding between the molecules will induce more possibility for aggregate growth, which in turn results in less ordered aggregate structures. It is worth noting that the size- as well as morphology-adjustable nanomaterials are highly desired for fabricating nanoscale molecular (opto) electronic devices which often require a wide variety of channel lengths to achieve the optimum gate or optical modulation.

Conclusion

In summary, we have devised, synthesized, and investigated the self-assembly properties of a series of mixed (phthalocyaninato)(porphyrinato) europium triple-decker complexes having different numbers of hydroxyl groups at the meso-attached phenyl groups of the porphyrin ligand. Comparative investigation results reveal that competition and/or cooperation of intermolecular hydrogen bondings with the $\pi-\pi$ interaction between tetrapyrrole rings in the triple-decker molecules leads to different molecular packing conformations and in turn different nanostructure morphologies in the self-assembly process. The $\pi-\pi$ interaction dominates the formation of nanostructures such as the nanoleafs and nanoribbons for **1** and **2**, while the dominant hydrogen bonding interaction in the direction perpendicular to the $\pi-\pi$ interaction direction leads to the nanosheets for **3** and nanospherical shapes for **5**. The balance between these two interactions among the triple-decker tetrapyrrole molecules also induces the formation of curved nanosheets for complex **4**, in which the long-range periodicity along the direction of $\pi-\pi$ interaction is still revealed. The result presented here represents the first effort toward realizing control over the self-assembled nanostructures of sandwich tetrapyrrole rare earth complexes through molecular design and synthesis. They are believed to be helpful in opening new possibilities for construction of molecular-based nano- and optoelectronics.

Experimental Section

TCB was distilled from anhydrous CaH_2 under reduced pressure prior to use. Column chromatography was carried out on silica gel (Merck, Kieselgel 60, 200−300 mesh) with the indicated eluent. All other reagents and solvents were of reagent grade and used as received. The compounds H_2TBPP,[40] H_2T(OH)PP,[41] H_2[*trans*-T(OH)$_2$PP],[42] H_2[*cis*-T(OH)$_2$PP],[41] H_2T(OH)$_3$PP,[41] Eu(acac)$_3$·nH$_2$O,[43] and EuPc$_2$[44] were prepared according to literature methods. A series of five triple-decker complexes, Eu$_2$(Pc)$_2$(TBPP) (**1**), Eu$_2$(Pc)$_2$[T(OH)PP] (**2**), Eu$_2$(Pc)$_2$[trans-T(OH)$_2$PP] (**3**), Eu$_2$(Pc)$_2$[cis-T(OH)$_2$PP] (**4**), and Eu$_2$(Pc)$_2$[T(OH)$_3$PP] (**5**), were prepared according to the reported procedure as detailed below.[30c]

The nanostructures of the five triple-decker compounds **1**−**5** were fabricated by the phase transfer method according to the following procedure.[20,21,23,45] A minimum volume (30−50 μL) of concentrated chloroform solution of compounds (**1**−**5**) (1 mM) was injected rapidly into 1 mL of *n*-hexane. This clear solution was used to record the electronic absorption spectra for the aggregates. It is worth noting that the electronic absorption spectra of these five triple-decker complexes in *n*-hexane do not change significantly along with the increase of the quiescent time of the solution until after 8 h at room temperature (25 °C). After being kept at room temperature for 24 h, precipitates were observed in the solution. These precipitates were transferred to the carbon-coated grid or mica by pipetting for the SEM and AFM observations. These procedures and results were reproducible under the experimental conditions described above.

Electronic absorption spectra were recorded on a Hitachi U-4100 spectrophotometer. MALDI-TOF mass spectra were carried out on a Bruker APEX47e ultrahigh resolution. A Fourier transform ion cyclotron resonance (FT-IR) mass spectrometer was utilized with α-cyano-4-hydroxycinnamic acid as the matrix for IR spectra. Elemental analyses were performed by the Institute of Chemistry, Chinese Academy of Sciences. ^{1}H NMR spectra were measured on a Bruker DPX 400 spectrometer (400 MHz) in $CDCl_3$. Low-angle X-ray diffraction (XRD) measurements were carried out on a Rigaku D/max-cB X-ray diffractometer. SEM images were obtained using a JEOL JSM-6700F field-emission scanning electron microscopy. AFM images were collected in air under ambient conditions using the tapping mode with a NanoscopeIII/Bioscope scanning probe microscope from Digital instruments. For SEM imaging, Au (1−2 nm) was sputtered onto the grids to prevent charging effects and to improve image clarity. For AFM imaging, the sample was cast onto a mica surface.

General Procedure for the Preparation of Eu$_2$(Pc)$_2$(Por) (1−5). A mixture of Eu(acac)$_3$·nH$_2$O (23 mg, 0.05 mmol), Eu(Pc)$_2$ (59 mg, 0.05 mmol), and H_2Por (0.05 mmol) was mixed in TCB (6 mL) and heated to reflux for 7 h. The volatiles were removed under reduced pressure, and the residue was chromatographed with $CHCl_3$ as eluent. A small amount of unreacted Eu(Pc)$_2$ and metal-free Porphyrin were collected as the first and second fractions, respectively, and then the target mixed ring triple-decker product Eu$_2$(Pc)$_2$(Por) (**1**−**5**) was collected as the third fraction. Repeated chromatography followed by recrystallization from $CHCl_3$ and *n*-hexane gave pure compounds Eu$_2$(Pc)$_2$(Por) (**1**−**5**) as a darkish-blue solid.

Acknowledgment. Financial support from the Natural Science Foundation of China, Ministry of Education of China, and Shandong University is gratefully acknowledged.

Supporting Information Available: IR spectra of compounds **1**−**5** in the region 400−4000 cm^{-1} with 2 cm^{-1} resolution, schematic representation of the unit cell in the aggregate of Eu$_2$(Pc)$_2$(TBPP) (**1**), ^{1}H NMR spectroscopic data (δ) for the triple-deckers **1**−**5** recorded in $CDCl_3$, electronic absorption data for the triple-deckers **1**−**5** in $CHCl_3$ and their self-assemblies in *n*-hexane. This material is available free of charge via Internet at http://pubs.acs.org.

JA802493V

(40) Bian, Y.; Jiang, J.; Tao, Y.; Choi, M. T. M.; Li, R.; Ng, A. C. H.; Zhu, P.; Pan, N.; Sun, X.; Arnold, D. P.; Zhou, Z.; Li, H.-W.; Mak, T. C. W.; Ng, D. P. K. *J. Am. Chem. Soc.* **2003**, *125*, 12257–12267.
(41) Little, R. G. *J. Heterocycl. Chem.* **1978**, *15*, 203–208.
(42) Littler, B. J.; Ciringh, Y.; Lindsey, J. S. *J. Org. Chem.* **1999**, *64*, 2864–2872.
(43) Stites, J. G.; McCarty, C. N.; Quill, L. L. *J. Am. Chem. Soc.* **1948**, *70*, 3142–3143.
(44) Jiang, J.; Liu, R. C. W.; Mak, T. C. W.; Chan, T. W. D.; Ng, D. K. P. *Polyhedron* **1997**, *16*, 515–520.
(45) Gong, X.; Milic, T.; Xu, C.; Batteas, J. D.; Drain, C. M. *J. Am. Chem. Soc.* **2002**, *124*, 14290–12491.